Boundary-Layer Meteorol (2007) 122:167–187
DOI 10.1007/s10546-006-9093-1

ORIGINAL PAPER

# Utility of radiometric–aerodynamic temperature relations for heat flux estimation

**William P. Kustas · Martha C. Anderson · John M. Norman · Fuqin Li**

Received: 8 August 2005/Accepted: 27 April 2006 /
Published online: 7 July 2006


**Abstract** In many land-surface models using bulk transfer (one-source) approaches, the application of radiometric surface temperature observations in energy flux computations has given mixed results. This is due in part to the non-unique relationship between the so-called aerodynamic temperature, which relates to the efficiency of heat exchange between the land surface and overlying atmosphere, and a surface temperature measurement from a thermal-infrared radiometer, which largely corresponds to a weighted soil and canopy temperature as a function of radiometer viewing angle. A number of studies over the past several years using multi-source canopy models and/or experimental data have developed simplified methods to accommodate radiometric–aerodynamic temperature differences in one-source approaches. A recent investigation related the variability in the radiometric–aerodynamic relation to solar radiation using experimental data from a variety of landscapes, while another used a multi-source canopy model combined with measurements over a wide range in vegetation density to derive a relationship based on leaf area index. In this study, simulations by a detailed multi-source soil–plant–environment model, Cupid, which considers both radiative and turbulent exchanges across the soil–canopy–air interface, are used to explore the radiometric–aerodynamic temperature relations for a semi-arid shrubland ecosystem under a range of leaf area/canopy cover, soil moisture and meteorological conditions. The simulated radiometric-aerodynamic temperatures indicate that, while solar radiation and leaf area both strongly affect the magnitude of this temperature difference, the relationships are non-unique, having significant variability depending on local conditions. These simulations also show that soil–canopy temperature differences are highly correlated with variations in the radiometric–aerodynamic temperature differences, with the slope being primarily a func-

W. P. Kustas (✉)· M. C. Anderson · F. Li
USDA-ARS Hydrology and Remote Sensing Laboratory, Bldg. 007, BARC-West, Beltsville, MD, USA
e-mail: bkustas@hydrolab.arsusda.gov

J. M. Norman
Department of Soil Science, University of Wisconsin, Madison, WI, USA

tion of leaf area. This result suggests that two-source schemes with reliable estimates of component soil and canopy temperatures and associated resistances may be better able to accommodate variability in the radiometric–aerodynamic relation for a wider range in vegetated canopy cover conditions than is possible with one-source schemes. However, comparisons of sensible heat flux estimates with Cupid using a simplified two-source model and a one-source model accommodating variability in the radiometric-aerodynamic relation based on vegetation density gave similar scatter. On the other hand, with experimental data from the shrubland site, the two-source model generally outperformed the one-source scheme. Clearly, vegetation density/leaf area has a major effect on the radiometric–aerodynamic temperature relation and must be considered in either one-source or two-source formulations. Hence these adjusted one-source models require similar inputs as in two-source approaches, but provide as output only bulk heat fluxes; this is not as useful for monitoring vegetation conditions.

**Keywords** Aerodynamic temperature · Heat flux estimation · One-source modelling · Radiometric temperature · Remote sensing · Two-source modelling

## 1 Introduction

Remote sensing-based land-surface models are one of the few techniques available for estimating spatially-distributed land-surface fluxes from local to regional scales. Over the past several decades, many different types of modelling systems have been developed to use remote sensing inputs for surface flux estimation (Kustas and Norman, 1996). A key boundary condition for many of these models is a directional radiometric surface temperature, $T_R(\phi)$, at viewing angle $\phi$. To simplify modelling requirements, $T_R(\phi)$ is often used to replace the so-called "aerodynamic temperature for heat", $T_O$ (K), which satisfies the bulk resistance formulation for sensible heat transport, $H$,

$$H = \rho C_P \frac{(T_O - T_A)}{R_A + R_{EX}} = \rho C_P \frac{(T_O - T_A)}{R_{AH}}, \tag{1}$$

where $H$ is the sensible heat flux (W m$^{-2}$), $\rho$ is air density (kg m$^{-3}$), $C_p$ is the heat capacity of air (J kg$^{-1}$ K$^{-1}$), $T_A$ is the air temperature in the surface layer measured at some height above the canopy (K), $R_{EX}$ is an excess resistance associated with heat transport (s m$^{-1}$), $R_A$ is the aerodynamic resistance (s m$^{-1}$), which has the following form in the surface layer (Brutsaert, 1982):

$$R_A = \frac{\left[\ln\left(\frac{z_U - d_O}{z_{OM}}\right) - \Psi_M\right]\left[\ln\left(\frac{z_T - d_O}{z_{OM}}\right) - \Psi_H\right]}{k^2 u} \tag{2}$$

and $R_{AH} \equiv R_A + R_{EX}$ is the total resistance to heat transport across the temperature difference $T_O - T_A$. In Eq. 2 $d_O$ is the displacement height, $u$ is the wind speed measured at height $z_U$, $k$ is von Karman's constant ($\approx 0.4$), $z_T$ is the height of the $T_A$ measurement, $\Psi_M$ and $\Psi_H$ are the Monin-Obukhov stability functions for momentum and heat, respectively, and $z_{OM}$ is the aerodynamic roughness length. In general, potential temperature should be substituted in Eq. (1), although when $z_T < 10$ m, the error in using actual temperatures is minor, except under stable conditions (Mahrt and Vickers 2004).

The excess resistance term embodies the fact that heat must diffuse through laminar boundary layers surrounding canopy and soil elements, while momentum is transferred more efficiently as a result of viscous shear and form drag of the roughness elements involving local pressure gradients. This difference in transport mechanisms for heat and moment is often expressed as a difference in effective roughness length: $R_{EX} = [\ln(z_{OM}/z_{OH})]/[ku_*]$, where $z_{OH}$ is the roughness length for heat transport and $u_*$ is the friction velocity; $u_* = uk/[\ln(z_U - d_O)/z_{OM} - \Psi_M]$, and $z_{OH}$ is typically of order 0.1 $z_{OM}$. Much effort has been expended to evaluate $z_{OH}$ or the ratio $\ln(z_{OM}/z_{OH}) = kB^{-1} = ku_* R_{EX}$ (Garratt and Hicks 1973) for different surfaces by using $T_R(\phi)$ observations and measurements of most of the variables in Eqs. (1) and (2). When $T_R(\phi)$ is used in Eq. (1) instead of $T_O$ with measured fluxes to estimate roughness, the conceptual framework defining $z_{OH}$ is revised to yield the so-called "radiometric roughness length" $z_{OR}$ (e.g., Brutsaert and Sugita 1996).

Studies evaluating $z_{OR}$ find considerable scatter in derived values and no single formulation that clearly explains the observed variability, particularly for partial canopies (e.g., Stewart et al. 1994; Sun and Mahrt 1995; Kustas et al. 1996; Verhoef et al. 1997; Troufleau et al. 1997). There are a significant number of factors that make it difficult to develop a unified theory that incorporates the many influences on $z_{OR}$. Blyth and Dolman (1995), using a two-source modelling approach that treats the land surface as a composite of soil and canopy elements, demonstrate the dependence of $z_{OH}(z_{OR})$ on various surface conditions including fractional vegetation cover, soil and vegetation resistances , as well as on the available energy or net radiation less soil heat flux (i.e., $R_N - G$), and humidity deficit. A similar result was obtained by Lhomme et al. (1997) using the two-source model originally developed by Shuttleworth and Wallace (1985). Moreover, observational and modelling studies show a dependency of $z_{OR}$ on radiometer viewing angle, $\phi$ (Vining and Blad 1992; Matsushima and Kondo 1997).

Despite the utility (in terms of physical fidelity) of describing the surface as two sources, there remains considerable interest in the meteorological community for improving one-source models. This is mainly due to the fact that most large-scale numerical model formulations of land-atmosphere heat transport involve solving Eq. 1. Consequently, many in the land-surface modelling and thermal remote sensing communities have focused on developing simple schemes to accommodate the inherent differences between $T_R(\phi)$ and $T_O$.

Some have examined approaches that avoid parameterization of $z_{OR}$ [e.g., assuming $R_{EX} = 0$ or a constant in Eq. (1)], and instead use semi-empirical formulations to account for the difference between $T_O$ and $T_R$ which, it is argued, can be more accurately applied to observations (e.g., Lhomme et al. 1994; Chehbouni et al. 1996, 1997; Mahrt et al. 1997; Sun et al. 1999). However, these formulations are typically calibrated with experimental data, and hence may not be generally applicable, making it difficult to apply a priori to different land cover types (Merlin and Chehbouni 2004).

A recent study using airborne flux and radiometric temperature data over eight different landscapes found a significant relationship between $T_R(\phi) - T_O$ and solar radiation, $S$, and leaf area index (LAI) (Mahrt and Vickers 2004). Simple linear expressions were used to describe these relationships, namely

$$T_R(\phi) - T_O = C\,(S - S_{crit}) \tag{3a}$$

$$S_{crit} = C_S(\mathrm{LAI} - \mathrm{LAI}_{ref}), \tag{3b}$$

for LAI > 1, where $C, S_{\text{crit}}$ and $C_S$ were derived from linear regression and $\text{LAI}_{\text{ref}}$ is approximately 1.0 (Mahrt and Vickers 2004). Even with land-cover conditions ranging from bare soil and crops to grassland and several types of forests, there was little variation in the value of $C$ (with an average value of 0.0087 K m$^2$ W$^{-1}$), suggesting this type of an approach may provide a more general formulation in accommodating differences between $T_R(\phi)$ and $T_O$ for different landscapes.

Others have derived formulations that adjust for $T_R(\phi) - T_O$ based on complex physical models of the soil–canopy heat exchange (e.g., Blümel 1999; Massman 1999; Su et al. 2001; Matsushima 2005). These modified one-source schemes require vegetation structure, density/leaf area, and other inputs similar to two-source models, and can compute sensible heat flux as reliably as two-source estimates over partial canopy covers (Su et al. 2001). However, for the same input needs as two-source approaches, these 'adjusted' one-source schemes provide less output information, namely bulk heat fluxes as opposed to fluxes partitioned between soil and canopy.

Matsushima (2005) developed a general parameterization to account for the variability in $T_R(\phi) - T_O$ based on multi-source canopy model simulations and experimental data over a rice paddy under a wide range of vegetation density conditions. Matsushima (2005) shows how $z_{OR}$ is analytically related to the $T_R(\phi) - T_O$ 'adjustment' formulations proposed originally by Chehbouni et al. (1996) and Troufleau et al. (1997). The adjustment to the one-source formulation originally proposed by Troufleau et al. (1997) is expressed by Matsushima (2005) in resistance form as

$$H = \rho C_P (1 - \alpha) \frac{T_R(\phi) - T_A}{R_{AH}}, \tag{4}$$

where $\alpha$ is defined as follows:

$$\alpha = \frac{T_R(\phi) - T_O}{T_R(\phi) - T_A}. \tag{5}$$

With the evaluation of Eqs. 4–5 using the multi-source canopy model simulations and the experimental data, Matsushima (2005) finds a relationship between $\alpha$ and vegetation density as quantified by LAI, which does not appear to be strongly affected by view angle effects.

In the study presented here, the comprehensive soil–plant–environment, Cupid (Norman and Campbell 1983; Norman and Arkebauer 1991; Kustas et al. 2004), which simulates radiation exchange, turbulent fluxes, and $T_R(\phi)$ and $T_O$ for plant canopies, will be used to simulate soil, canopy, radiometric and aerodynamic temperatures for a semi-arid rangeland/ shrubland ecosystem under a wide range of meteorological, soil moisture and vegetation cover (LAI) conditions. The resulting predictions of $T_R(\phi)$ and $T_O$ will be used to assess the generality of simple empirical approaches such as that in Eqs. (3) and (5). In addition, the one-source approaches described above that adjust for $T_R(\phi) - T_O$ based on LAI and other inputs similar to a simplified two-source model that implicitly accommodates for this difference, will be compared to Cupid-simulated sensible heat fluxes and the experimental data collected from this semi-arid rangeland/shrubland site.

## 2 Methods

### 2.1 Cupid model description and applications

Cupid is a detailed, multi-source soil–plant–environment model that simulates a wide variety of physiological and environmental processes simultaneously. The canopy is divided into numerous horizontal layers, and leaves in each layer are arranged with appropriate position and orientation distributions. Transfer of energy, mass and momentum is assumed to occur only in the vertical dimension, and this transport is described by turbulent diffusion with leaves in each layer acting as sources or sinks of various quantities (Norman 1979, 1988). Recently an analytical Lagrangian theory approach has been implemented in Cupid (Wilson et al. 2003). The below-ground transport of heat and mass provides a description of the soil environment that surrounds the roots and incorporates the exchanges between these roots and the soil system.

The Cupid model simulates processes occurring at the soil/canopy interface, including absorption of radiation and momentum by the soil surface, convective transport of heat and water from the soil and vegetation to the atmosphere, conduction of heat and water from lower in the soil to the surface, uptake of water by roots near the soil surface, and infiltration of rainfall, irrigation water, or water that drips from the canopy as a result of interception. The leaf model combines the response of photosynthetic rate and stomatal conductance to micrometeorological factors and is described in Norman and Polley (1989).

Canopy exchange rates are estimated by combining equations that describe leaf-level processes with a characterization of canopy architecture, boundary measurements of ambient environment above the canopy and below the root zone, and with equations that describe convective, conductive and radiative exchange processes throughout the soil–plant–atmosphere system. A description of canopy architecture includes the vertical distribution of stem and leaf area, leaf angle distribution, canopy height, and information about the horizontal distribution of leaf area (e.g., random or clumped). Many canopies are clumped, particularly forests, and Cupid handles these situations with a clumping factor approach that has been well studied (Chen et al. 1997). Ambient atmospheric conditions are input to the model at every time-step, using measurements of air temperature, humidity, wind speed, solar radiation and precipitation some metres above the canopy. If not measured, incoming thermal radiation from the sky is estimated from air temperature and humidity (Brutsaert 1975). Ambient soil boundary conditions of temperature and moisture content near the bottom of the root zone (0.5–2 m depth) must also be specified.

The influence of vertical gradients throughout the soil–plant–atmosphere system is included by using an iterative-solution technique that simultaneously solves the leaf energy budget for all leaves and the vertical flux-gradient equations. Such a solution requires that conductances be specified throughout the soil and atmospheric system; including aerodynamic conductances above and within the canopy, convective transfer coefficients at the soil surface, leaf boundary-layer conductances, and soil thermal and hydraulic conductances (Campbell 1985).

The Cupid model has been extensively tested with respect to many environmental variables. Surface flux predictions have been compared to measurements in potato crops (Wilsonet al. 2003) using both K-theory and Lagrangian turbulence theories, and also in cranberries (Bland et al. 1996). Leaf wetness, one of the most difficult quantities to predict, has been compared to measurements in potatoes (Wilson et al. 1999; Wilson et al. 2003) in Wisconsin and dry edible beans (Weiss et al. 1989) in western Nebraska with good results. Interception of irrigation water by leaves was predicted and measured in corn in Kansas with reasonable results (Norman and Campbell 1983). Radiation penetration predictions have been compared to measurements in corn (Norman, 1988) and a Sitka Spruce forest (Norman and Jarvis 1975). Bidirectional reflectance factors estimated from Cupid have been compared to remote-sensing measurements in soybeans (Norman et al. 1985). Net $CO_2$ measurements from photosynthesis and respiration have been compared to Cupid estimates for a Kansas native prairie (Norman and Polley 1989), cranberry (Bland et al. 1996) and potato (Wilson et al. 2003). Clearly the Cupid model has undergone testing of many of the quantities that have a major influence on soil and vegetation temperatures.

Furthermore, simplified canopy models for estimating canopy transpiration, carbon assimilation (ALEX-Atmosphere Land Exchange; Anderson et al. 2000) and surface energy fluxes using radiometric surface temperature (TSM - Two-Source Model; Norman et al. 1995) have been developed from the analysis of numerous Cupid simulations and evaluated with experimental data over a wide variety of land cover (Anderson et al. 2000; Crow and Kustas 2005). The generally good performance in flux estimation with the simplified canopy models serve as further validation of key parameterizations used in Cupid.

The Cupid model is a useful platform for studying the relationship between aerodynamic temperature, $T_{\mathrm{O}}$, which is related to the sensible heat flux from a soil–canopy system (cf., Eq. (1) but cannot be measured directly, and the radiometric surface temperature, $T_{\mathrm{R}}(\phi)$, which can be measured with thermal-infrared radiometers and infrared thermometers. When combined with the surface-layer air temperature and a resistance calculated from Monin-Obukhov surface-layer similarity theory, the aerodynamic temperature provides an estimate of the surface sensible heat flux (Norman and Becker 1995). The radiometric temperature is based on the infrared radiance emanating from the soil–canopy system. The directional radiometric temperature, $T_{\mathrm{R}}(\phi)$, is calculated from the radiance measured by a narrow-field-of-view infrared radiometer, and is actually referred to as the "ensemble directional radiometric surface temperature", representing the collection of different surface elements present within the sensor footprint (Norman and Becker, 1995). The equations used in Cupid to calculate $T_{\mathrm{R}}(\phi)$ incorporate the effects for both vegetation and soil and have been outlined in Kustas et al. (2004). Furthermore, a comparison of model versus measured brightness temperatures demonstrating the validity of the Cupid algorithms can also be found in Kustas et al. (2004).

It is important to note that numerous surface temperatures can be defined (Norman and Becker 1995). Converting the raw, calibrated infrared thermometer measurement of brightness temperature to a directional radiometric temperature requires accounting for the variation in directional emissivity (Norman and Becker 1995). The directional emissivity of the soil/canopy system is calculated in the Cupid model (Kustas et al. 2004, Appendix A) as well as the soil/canopy system albedo using radiative transfer equations (Norman and Jarvis 1975). For further details on how Cupid computes both convective and radiative fluxes through the soil–canopy layers see Kustas et al. (2004) and the Web site http://www.soils.wisc.edu/~norman/cupid/, where documentation and the Fortran code for running Cupid is available.

In Cupid, the aerodynamic temperature is computed by several methods, but the most widely accepted method is described by Eqs. (24) and (26) in Norman and Becker (1995), which is similar to Eq. (1). The calculation of sensible heat flux $H$ in Cupid, necessary to calculate aerodynamic surface temperature, is also described by Norman and Campbell (1983). In Cupid, the aerodynamic temperature for heat (based on $z_{0H}$) and for momentum (based on $z_{0M}$) are both calculated. The aerodynamic roughness length is a required input parameter for Cupid that is calculated as a fraction of vegetation height, varying from 0.05 to 0.2, and vegetation type. The roughness length for heat ($z_{0H}$) is also calculated in Cupid.

## 2.2 Cupid model validation with Monsoon '90 data

Cupid model output was compared with measurements from the Lucky Hills site (Site 1) of the Monsoon 90 experiment (Kustas and Goodrich 1994) including the energy balance components, the component temperatures of the vegetation and soil, the canopy/soil emissivity, and the soil-surface evaporation rate. Soil, canopy and weather inputs for the Cupid model were obtained from published measurements for the Monsoon 90 experiment (see Kustas et al. 2004). Lucky Hills contains sparse and clumped shrubland vegetation conditions that are most problematic for one-source models and for developing a general parameterization of $z_{OH}$ or $z_{OR}$. Although sparsely vegetated, the shrubs do significantly reduce wind speed near the soil surface, and hence reduce the efficiency of heat transport from the soil. On the other hand, the shrub canopy is highly efficient at heat exchange. The $T_R(\phi)$ observations have a much stronger temperature signal from the soil surface relative to the canopy elements; consequently, it is essential that the model consider the disparate efficiencies in heat transport from the canopy and soil components (Norman et al. 1995). This type of landscape is therefore a significant challenge for the application of bulk-transfer or one-source models.

In Kustas et al. (2004), micrometeorological measurements of the primary energy balance flux components of net radiation, $R_N$, soil heat flux, $G$, sensible heat flux, $H$, and latent heat flux, LE (Stannard et al. 1994) were compared to Cupid predictions over a two-week period spanning very dry to wet surface soil moisture conditions. Root-mean-square difference (RMSD) values (Willmott 1982) were relatively low at 20, 25, 30 and 40 W m$^{-2}$ for $R_N, G, H$ and LE, respectively. Measurements of component soil and canopy temperatures and soil and canopy evaporative fluxes were also compared to Cupid output and yielded good agreement. The RMSD values were 2.3 and 0.9 K, and 13 and 37 W m$^{-2}$ for soil and vegetated canopy temperatures, and latent heat fluxes, respectively (see Kustas et al. 2004 for details).

## 2.3 Cupid model simulations using Monsoon '90 data

With the validated Cupid model for the semi-arid shrubland site, brightness temperature, radiometric and aerodynamic temperatures were simulated for 36 cases: two radiometer view angles ($\phi = 0°$ or nadir and 55°), two wind speeds (1 and 5 m s$^{-1}$), three cover conditions reflecting water availability in the typical upland (LAI = 0.5), mid slope (LAI = 1.5) and low elevation/riparian areas (LAI = 3.0), unstressed vegetation with a dry soil surface, unstressed vegetation with a moist soil surface, and stressed vegetation with a dry soil surface. Table 1 is a summary of the different cases simulated by Cupid. The two radiometer view angles cover the range of usable satellite-based $T_R(\phi)$ data, and in particular the viewing angles of the directional thermal-infrared sensors from the Advanced Along Track Scanning Radi-

**Table 1** Linear regression coefficients and correlation ($r$) between Cupid simulated radiometric–aerodyanmic temperature difference ($T_R(\phi) - T_O$) and solar radiation ($S$) for the 36 cases using the equation developed by Marht and Vickers (2004)

| Leaf area index | Plant stress | Soil surface wetness | Wind ($m\,s^{-1}$) speed | $\phi$ (degrees) | Slope $C$ ($K/(W\,m^{-2})$) | $S_{crit}$ ($W\,m^{-2}$) | $r$ |
|---|---|---|---|---|---|---|---|
| 0.5 | Unstressed | Wet | 1 | 0 | 0.0065 | 129 | 0.98 |
| | | | | 55 | 0.0056 | 120 | 0.98 |
| 1.5 | Unstressed | Wet | 1 | 0 | 0.0046 | 268 | 0.95 |
| | | | | 55 | 0.0032 | 250 | 0.95 |
| 3.0 | Unstressed | Wet | 1 | 0 | 0.0020 | 21 | 0.85 |
| | | | | 55 | 0.0015 | −21 | 0.80 |
| 0.5 | Unstressed | Wet | 5 | 0 | 0.0056 | −315 | 0.70 |
| | | | | 55 | 0.0049 | −324 | 0.69 |
| 1.5 | Unstressed | Wet | 5 | 0 | 0.0061 | −388 | 0.99 |
| | | | | 55 | 0.0041 | −387 | 0.99 |
| 3.0 | Unstressed | Wet | 5 | 0 | 0.0017 | −376 | 0.98 |
| | | | | 55 | 0.0007 | −315 | 0.97 |
| 0.5 | Unstressed | Dry | 1 | 0 | 0.0189 | 163 | 0.99 |
| | | | | 55 | 0.0163 | 160 | 0.99 |
| 1.5 | Unstressed | Dry | 1 | 0 | 0.0112 | 269 | 0.96 |
| | | | | 55 | 0.0069 | 304 | 0.95 |
| 3.0 | Unstressed | Dry | 1 | 0 | 0.0030 | 337 | 0.76 |
| | | | | 55 | 0.0010 | 455 | 0.37 |
| 0.5 | Unstressed | Dry | 5 | 0 | 0.0169 | 37 | 0.99 |
| | | | | 55 | 0.0145 | 35 | 0.99 |
| 1.5 | Unstressed | Dry | 5 | 0 | 0.0114 | 108 | 0.99 |
| | | | | 55 | 0.0073 | 121 | 0.98 |
| 3.0 | Unstressed | Dry | 5 | 0 | 0.0027 | 104 | 0.96 |
| | | | | 55 | 0.0008 | 218 | 0.96 |
| 0.5 | Stressed | Dry | 1 | 0 | 0.0228 | 90 | 0.99 |
| | | | | 55 | 0.0199 | 85 | 0.99 |
| 1.5 | Stressed | Dry | 1 | 0 | 0.0140 | 42 | 0.96 |
| | | | | 55 | 0.0097 | −17 | 0.95 |
| 3.0 | Stressed | Dry | 1 | 0 | 0.0070 | −216 | 0.86 |
| | | | | 55 | 0.0043 | −458 | 0.83 |
| 0.5 | Stressed | Dry | 5 | 0 | 0.0174 | 46 | 0.99 |
| | | | | 55 | 0.0150 | 49 | 0.99 |
| 1.5 | Stressed | Dry | 5 | 0 | 0.0100 | 131 | 0.99 |
| | | | | 55 | 0.0060 | 173 | 0.99 |
| 3.0 | Stressed | Dry | 5 | 0 | 0.0003 | 2680 | 0.36 |
| | | | | 55 | -0.0018 | −345 | −0.98 |

See Eq. (3a, b)

ometer (www.le.ac.uk/ph/research/eos/aatsr/). Some of the input values describing the basic aerodynamic characteristics of the surface are listed in Table 2.

For meteorological inputs to the model, local weather data for a clear day at Lucky Hills during the field campaign on 28 July 1990 were used (except for the wind speed); the solar radiation, $S$, varied from 120 to 990 $W\,m^{-2}$, the vapour pressure varied from 0.85 to 1.25 kPa, and the air temperature, $T_A$, varied from approximately 28.4 to 31.5°C. These variables were measured at nominally 4 m above the local topography.

There is observational and conceptual/theoretical support for assuming non-equivalence between $z_{OH}$ and $z_{OM}$ for plant canopies (Brutsaert 1982; McNaughton and van den Hurk 1995; Massman 1999). However, to maintain consistency with the approach adopted by Marht and Vickers (2004), the values of the aerodynamic temperature, $T_O$, reported in the following were estimated using Eqs. (1) and (2) with $z_{OH} = z_{OM}$.

**Table 2** Some basic model inputs describing the aerodynamic characteristics of the different cover types used in the Cupid simulations (see Kustas et al. 2004 for details)

| LAI | Cover type | $h_C^a$(m) | $z_{OM}/h_C^b$ | $d_O/h_C^b$ | $f_C^c$ | $\Omega^d$ |
|---|---|---|---|---|---|---|
| 0.5 | Upland shrub | 0.5 | 0.16 | 0.44 | 0.28 | 0.7 |
| 1.5 | Midslope shrub | 0.5 | 0.09 | 0.71 | 0.55 | 0.7 |
| 3.0 | Lowland/riparian shrub | 0.5 | 0.07 | 0.79 | 0.80 | 1 |

[a] Canopy height

[b] ratio $z_{OM}/h_C$ and $d_O/h_C$ computed from LAI and the analytical model of Raupach (1994)

[c] Fractional vegetation (shrub) cover

[d] Clumping factor where $\Omega < 1$ indicates the vegetation (LAI) is not uniformly distributed over the landscape

Values of $T_O$ were also computed by Cupid using the ratio $z_{OH}/z_{OM} = 0.1$, typical for vegetated canopies (Brutsaert 1982) and used in assessing the Matsushima (2005) $\alpha$ parameter. Validation of either adjustment approach was not significantly influenced by whether $z_{0H}/z_{0M} = 0.1$ or 1.

## 3 Results and discussion

### 3.1 Cupid simulated $T_R(\phi) - T_O$ used with adjustment formulations

The Cupid-derived estimates of the near-surface temperature difference $T_R(\phi) - T_O$ for the 36 cases described above are plotted versus $S$ in Fig. 1(a,b) showing results for $\phi = 0°$ and $\phi = 55°$, respectively. The two wind speed conditions are not distinguished in these plots, so each symbol has two values for every value of $S$. Note the negative values of $T_R(\phi) - T_O$, which are predominately from wet soil conditions; this has also been observed in experimental data (Sun and Mahrt 1995).

It is clearly seen in Fig. 1 that there is a strong linear relationship between $S$ and $T_R(\phi) - T_O$ on a case-by-case basis. However, linear least squares regressions using Eq. (3a) yield a wide range in slope, $C$, and intercept values $S_{crit}$ across cases; *there is not one set of parameters that adequately describes the full range in surface conditions considered here*. In Table 1, the least squares regression fit with values of $C, S_{crit}$ and the correlation coefficient $r$ are listed for each of the 36 cases. Although in many cases $r > 0.95, C$ ranges from $-0.0018$ to $0.023\,\mathrm{K\,m^2\,W^{-1}}$ while $S_{crit}$ values are both positive and negative (not a realistic solution) ranging from –458 to $2680\,\mathrm{W\,m^{-2}}$. In comparison, Mahrt found that $C$ showed little variation with an average value of 0.0087. However, the range in $T_R(\phi) - T_O$ in this study (Fig. 1) is approximately $-10$ to 30 K whereas in Mahrt and Vickers (2004) the range was constrained, nominally $-3$ to 5 K—a very small segment of the possible range in variation. In addition, $C$ is also shown to vary with the radiometer view angle (see Table 1), which is not accounted for by the method.

The linear dependence between $S_{crit}$ and LAI for a subset of the data Mahrt and Vickers (2004) evaluated suggested a linear parameterization as described in Eq. (3b). The values of $S_{crit}$ vs. LAI estimated from Cupid are shown in Fig. 2. Any linear dependence that might exist for a single set of environmental and canopy cover conditions is obscured when a range in these conditions is considered. This suggests that simple parameterizations, such as in Eq. (3a, b), will not be very useful when applied to a wider range of landscape and meteorological conditions.

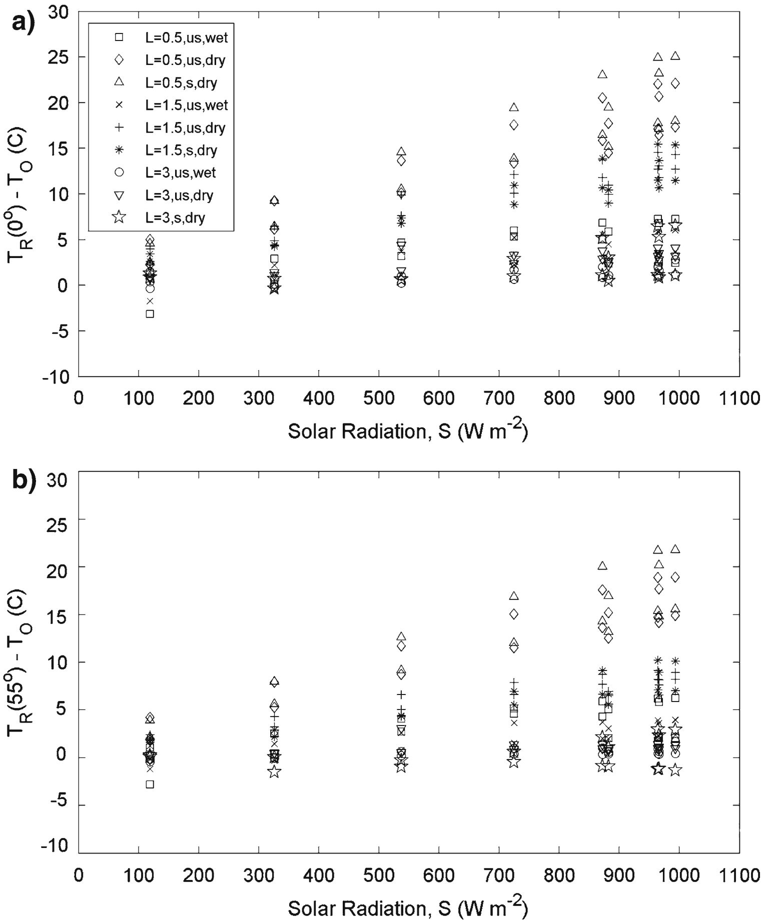


**Fig. 1** Comparison between Cupid simulated radiometric–aerodynamic temperature difference ($T_R(\phi) - T_O$) and solar radiation ($S$) for the different cases (L = LAI, us = unstressed vegetation, s = stressed vegetation, dry = dry soil surface moisture, wet = wet soil surface moisture) with radiometer view angle (**a**) $\phi = 0°$ and (**b**) $\phi = 55°$. Each symbol type contains a range of solar radiation, vapor pressure and air temperature values under the two wind speed conditions ($u = 1$ and $5\,\mathrm{m\,s^{-1}}$). See text for details

The values of $\alpha$ computed via Eq. (5) are illustrated in Fig. 3 along with the curve interpolated from the results in Matsushima (2005; Table 1). Although the curve goes through the points for the three LAI values, there is significant variation in the magnitude of $\alpha$, particularly for LAI = 3 condition. Again it does not appear as if this formulation, which is essentially a function of LAI, can adequately accommodate the variation in $T_R(\phi) - T_O$ caused by other canopy and meteorological factors.

## 3.2 Cupid simulated $T_R(\phi) - T_O$ versus soil–canopy temperature

### *3.2.1 Differences*

A comparison of $T_R(\phi) - T_O$ versus soil–canopy temperature differences, $T_S - T_C$, for the 18 cases with a nadir viewing angle ($\phi = 0°$) for the 18 cases with $\phi = 55°$ off

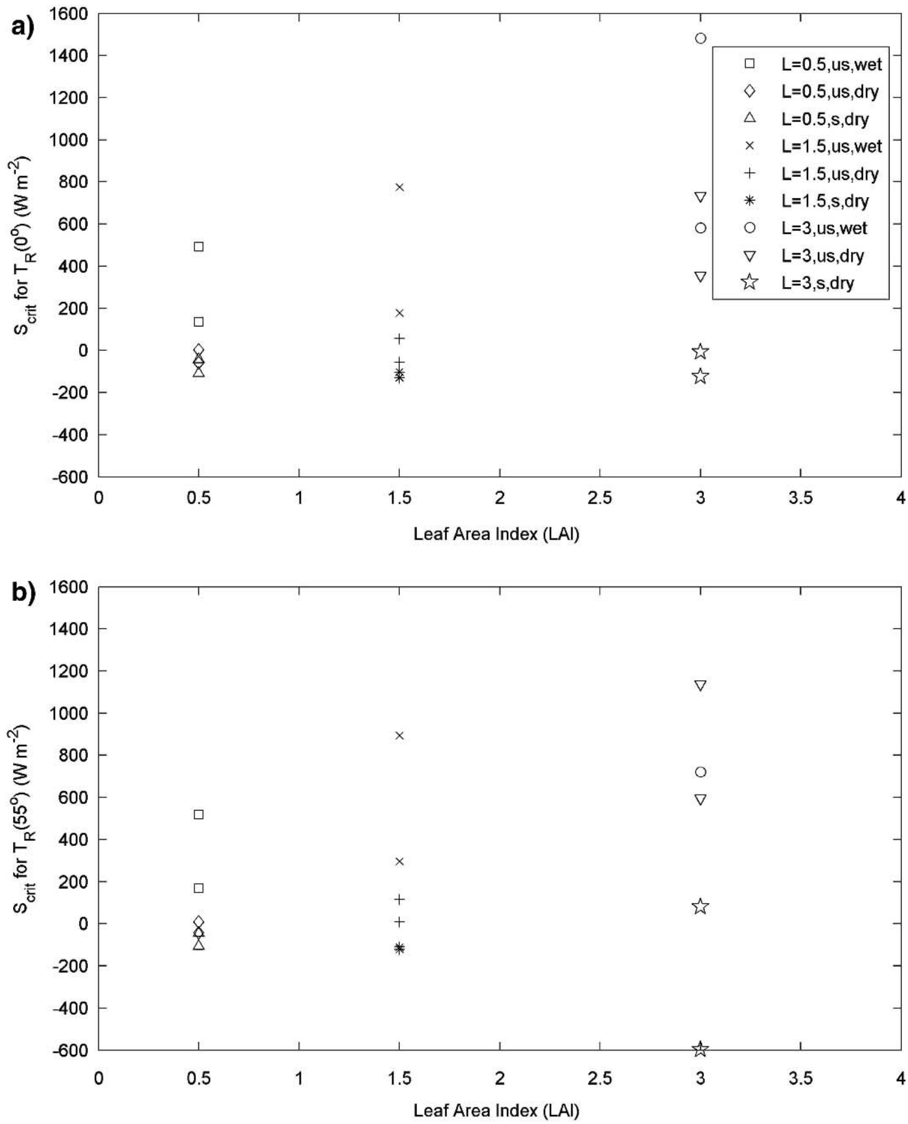


**Fig. 2** Values of $S_{crit}$ derived from Cupid simulated radiometric–aerodynamic temperature difference ($T_R(\phi) - T_O$) and least squares linear regression fit with solar radiation ($S$) via Eq. (3a) for the different cases as a function of LAI. Note that fitting Eq. (3b) to these data would require significantly different values of the slope, $C_S$. See text for details

nadir are illustrated in Fig. 4a, b, respectively. The $T_R(\phi) - T_O$ values collapse significantly compared to Fig. 1. For many of the cases, there is a strong linear relationship between $T_R(\phi) - T_O$ and $T_S - T_C$ ; however , the slope varies with stress and moisture condition supporting the simulations of Blyth and Dolman (1995). Moreover, comparing Fig. 2a, b, the slopes are also a function of the radiometer-viewing angle. In Table 3, the linear least squares regression fit between $T_R(\phi) - T_O$ and $T_S - T_C$ are given

**Table 3** Linear regression coefficients and correlation, $r$, between Cupid simulated radiometric–aerodynamic temperature difference ($T_R(\phi) - T_O$) and soil–canopy temperature differences ($T_S - T_C$) in the form $T_R(\phi) - T_O = a(T_S - T_C) + b$

| Leaf area index | Plant stress | Soil wetness surface | Wind speed ($m\,s^{-1}$) | $\phi$ (degrees) | Slope $a(-)$ | Intercept $b$(C) | $r$ |
|---|---|---|---|---|---|---|---|
| 0.5 | Unstressed | Wet & dry | 1 & 5 | 0° | 0.765 | −0.416 | 0.99 |
| | & stressed | | | 55° | 0.662 | −0.395 | 0.99 |
| 1.5 | Unstressed | Wet & dry | 1 & 5 | 0° | 0.554 | 0.036 | 0.99 |
| | & stressed | | | 55° | 0.345 | 0.088 | 0.98 |
| 3.0 | Unstressed | Wet & dry | 1 & 5 | 0° | 0.268 | 0.052 | 0.68 |
| | & stressed | | | 55° | 0.060 | 0.139 | 0.24 |

for three canopy cover cases (i.e., LAI = 0.5, 1.5 and 3) but include both stress and unstressed vegetation, dry and wet surface soil moisture and the 1 and 5 $m\,s^{-1}$ wind speed conditions. Both the results in Fig. 4 and Table 3 indicate that for the higher vegetation cover case, LAI = 3, there is weaker correlation between $T_R(\phi) - T_O$ and $T_S - T_C$; also, $T_R(\phi) - T_O$ values are mainly within ±2 K.

These small temperature differences indicate that under high cover conditions, $T_R(\phi)$ and $T_O$ may be nearly equal , as has been observed experimentally for dense grassland cover (Sun 1999; Kustas et al. 2001), a dense coniferous forest (Bosveld et al., 1999), and a riparian area comprised of dense stands of tamarisk or salt cedar (Kustas et al. 2002). This suggests that the utility of separating soil and canopy temperatures under high vegetative cover conditions may prove difficult and unreliable. However, under high vegetative cover conditions, the need to separate soil and canopy temperatures is minimal if fluxes are of interest, because soil fluxes tend to be small.

The difference between radiometric and aerodynamic temperatures is highly variable and clearly indicates the challenge associated with any scheme for adjusting a one-source model for such differences. Two-source models, which compute a temperature in the canopy air space from component soil and vegetation temperatures and associated resistances, may be better able to capture important factors influencing the aerodynamic temperature. Consequently, two-source approaches provide a more direct means of accommodating radiometric–aerodynamic temperature differences when applied to heterogeneous landscapes (Anderson et al. 1997; Friedl 2002; Zhan et al. 1996).

### 3.3 One-and two-source model flux estimates versus cupid simulations and Monsoon ’90 measurements

The TSM scheme originally proposed by Norman et al. (1995) with modifications described by Kustas and Norman (1999) has been shown to reproduce the fluxes and temperatures from an earlier subset of the Cupid simulations presented here (i.e., using a significantly smaller range in conditions than in the present study) with reasonable accuracy (Kustas and Norman 2000; Kustas et al. 2004). A more thorough comparison of the TSM is made under the full range of conditions simulated with Cupid and compared with the one-source model (OSM) approach of Matsushima (2005) using the $\alpha$ adjustment for $T_R(\phi) - T_O$ illustrated in Fig. 3 (Eqs. 4 and 5). In

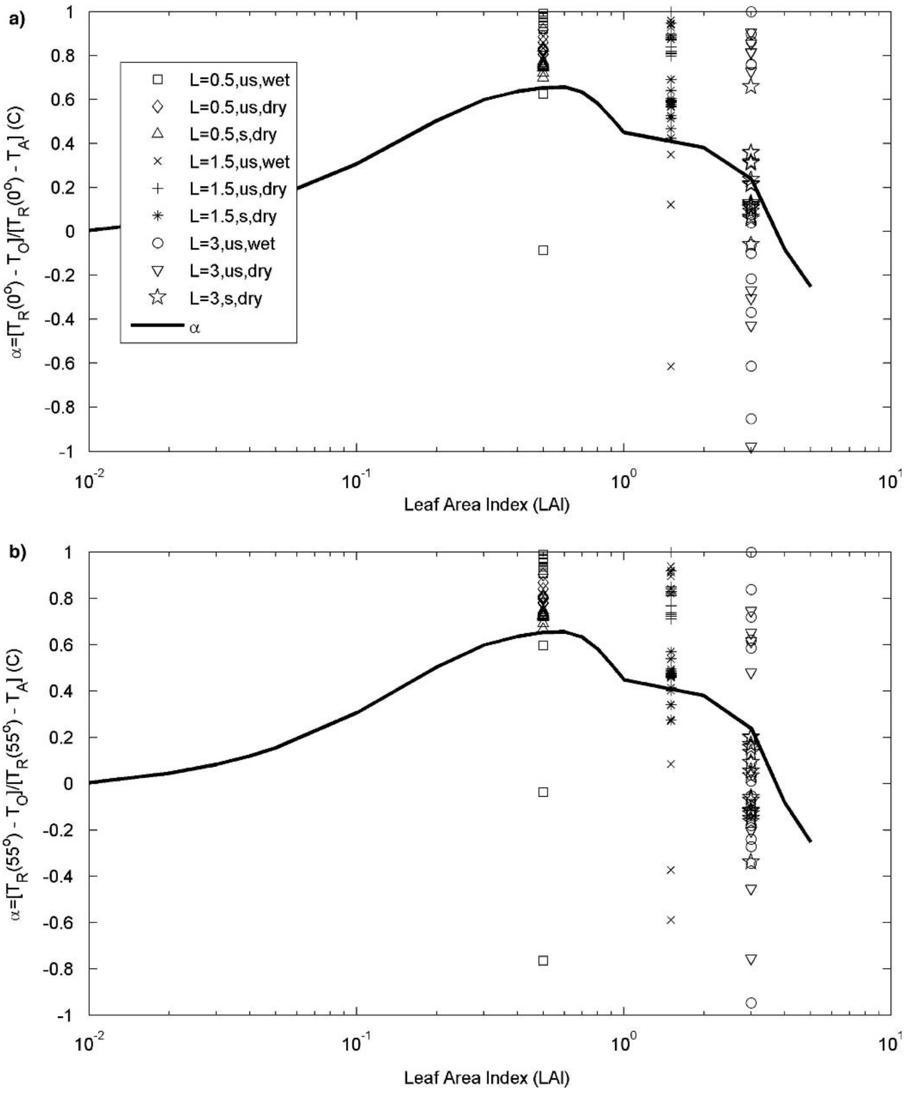


**Fig. 3** Values of $\alpha$ computed from Eq. (5) using the Cupid simulated $T_R(\phi)$ and $T_O$ for for the different cases (L = LAI, us = unstressed vegetation, s = stressed vegetation, dry = dry soil surface moisture, wet = wet soil surface moisture) with radiometer view angle (**a**) $\phi = 0°$ and (**b**) $\phi = 55°$. Each symbol type contains a range of solar radiation, vapour pressure and air temperature values under the two wind speed conditions ($u = 1$ and $5\,\mathrm{m\,s^{-1}}$). The curve (line) was fit to the results in Table 1 from Matsushima (2005). See text for details

addition, the Lucky Hills (Site 1) experimental data used in validating Cupid will be used to evaluate TSM and OSM sensible heat flux estimates. The roughness values used by TSM and OSM are given in Table 2, and for OSM $z_{0H}/z_{0M} = 0.1$. For Lucky Hills, the canopy height, LAI and roughness parameters are also defined in Table 2 for the upland shrub land cover type.

Application of Mahrt and Vickers (2004) adjustment to OSM, Eq. (3), with coefficients derived for the Cupid simulations and grouped by LAI gave inferior results.

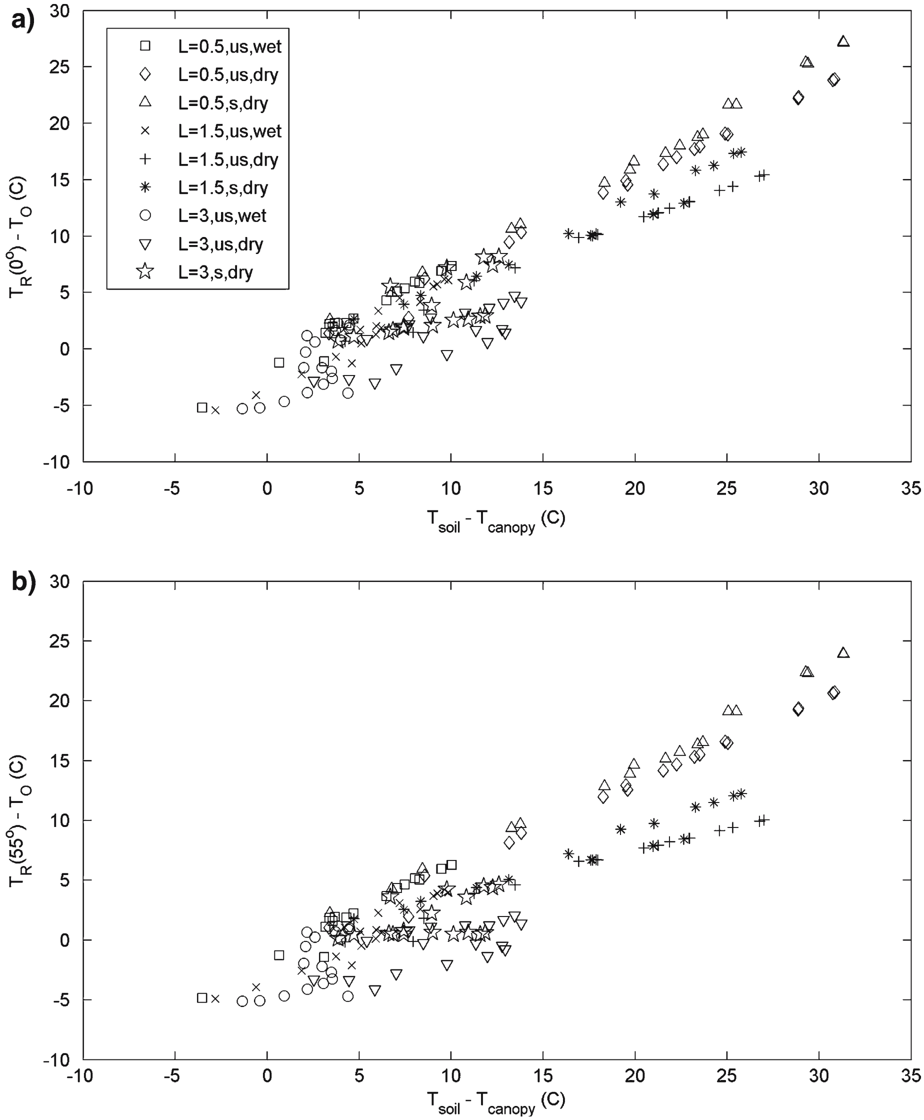


**Fig. 4** Comparison between Cupid simulated radiometric–aerodynamic temperature difference ($T_R(\phi) - T_O$) and soil–canopy temperature differences ($T_S - T_C$) for the different cases (L = LAI, us = unstressed vegetation, s = stressed vegetation, dry = dry soil surface moisture, wet = wet soil surface moisture) with radiometer view angle (**a**) $\phi = 0°$ and (**b**) $\phi = 55°$. Each symbol type contains a range of solar radiation, vapour pressure and air temperature values under the two wind speed conditions ($u = 1$ and $5\,\mathrm{m\,s^{-1}}$). See text for details

This approach was unable to compute physically meaningful solutions for nearly 25% of the Cupid simulated conditions, while the remaining simulated cases yielded a RMSD > $200\,\mathrm{W\,m^{-2}}$. With the Lucky Hills experimental data, physically plausible solutions were computed for almost all observations, but the RMSD was still unacceptable reaching nearly $200\,\mathrm{W\,m^{-2}}$. Hence, these results are not presented or contrasted to the TSM or other OSM approach.

The comparison of $H$ from Cupid simulations versus $H$ from TSM and OSM with $\alpha$ adjustment for $T_R(0°)$ is illustrated in Fig. 5. For both modelling schemes there are significant discrepancies with Cupid output, but surprisingly (given the scatter in the $\alpha$ variable in Fig. 3), the OSM scheme yields a similar RMSD value as the TSM, around 85 W m$^{-2}$. This is a fairly large RMSD; however, the Cupid simulations include extreme soil moisture and vegetation conditions, not often observed. The TSM has a larger mean bias of approximately 60 W m$^{-2}$ compared to the 25 W m$^{-2}$ for OSM, but TSM has a slightly higher $r^2(= 0.85)$ compared to OSM ($r^2 = 0.81$). If clumping of the vegetation, typical for shrubland sites (see Table 1), is considered, the effective LAI is reduced to ΩLAI, and changes the estimation of $\alpha$. However, there is little change in the results from including the clumping effect for OSM (not shown). Similarly, there were minor changes in the overall RMSD values when comparing both the TSM and OSM output of $H$ using $T_R(55°)$ with Cupid. Only for the OSM scheme did the viewing angle have a measurable affect on the heat flux computations, which was primarily under partial canopy cover (LAI = 0.5 and 1.5) with dry surface moisture and stressed vegetation conditions.

With the Lucky Hills data from Monsoon '90, the results comparing TSM and OSM $H$ output with flux observations are illustrated in Fig. 6. In this case, the TSM estimates agree more closely with the $H$ observations (RMSD ≈ 35 W m$^{-2}$) than OSM (RMSD ≈ 60 W m$^{-2}$). This is due in part, however, to the significant mean bias (underestimate) by OSM of ≈ 50 W m$^{-2}$ compared to the TSM bias of ≈ 20 W m$^{-2}$; the $r^2$ values are similar between TSM (= 0.79) and OSM (= 0.76). By including the clumping factor effect via Ω LAI(Ω = 0.7), the estimated $\alpha$ changes from 0.64 (for site LAI = 0.5) to 0.58 (for Ω LAI = 0.35). This reduces the RMSD to ≈ 50 W m$^{-2}$ and yields a smaller mean bias of ≈ 40 W m$^{-2}$. Other factors were found to significantly influence heat flux computations and bias with OSM. In particular, assuming $z_{0H}/z_{0M} = 1$, resulted in a mean bias of ≈ −5 W m$^{-2}$, but caused a much greater RMSD value of approximately 130 W m$^{-2}$. Clearly, the value assumed for $z_{0H}/z_{0M}$ has a significant effect on OSM approaches, even for those that adjust for radiometric–aerodynamic temperature differences.

## 4 Concluding remarks

This study indicates that the use of simple expressions to account for differences between radiometric and aerodynamic surface temperatures in the application of bulk-transfer or one-source models of heat exchange may not be widely applicable to diverse landscapes containing a variety of vegetation cover and soil moisture conditions. Past attempts to define radiometric–aerodynamic relations using experimental data have been found to be site and condition specific, although some studies have made progress by using complex physical canopy models to derive fairly simple methods to adjust one-source schemes for radiometric–aerodynamic temperature differences (e.g., Su et al. 2001; Matsushima 2005). These adjusted one-source models require similar inputs as two-source approaches, but provide only bulk heat fluxes as output, which is not as useful for assessing vegetation conditions.

Simulated radiometric and aerodynamic temperatures generated by a detailed multi-source soil–plant–environment model, Cupid, for a sparse, moderate and high fractional cover shrubland site for two wind speeds, dry and wet surface soil moisture, stressed and unstressed vegetation conditions and for two radiometer viewing

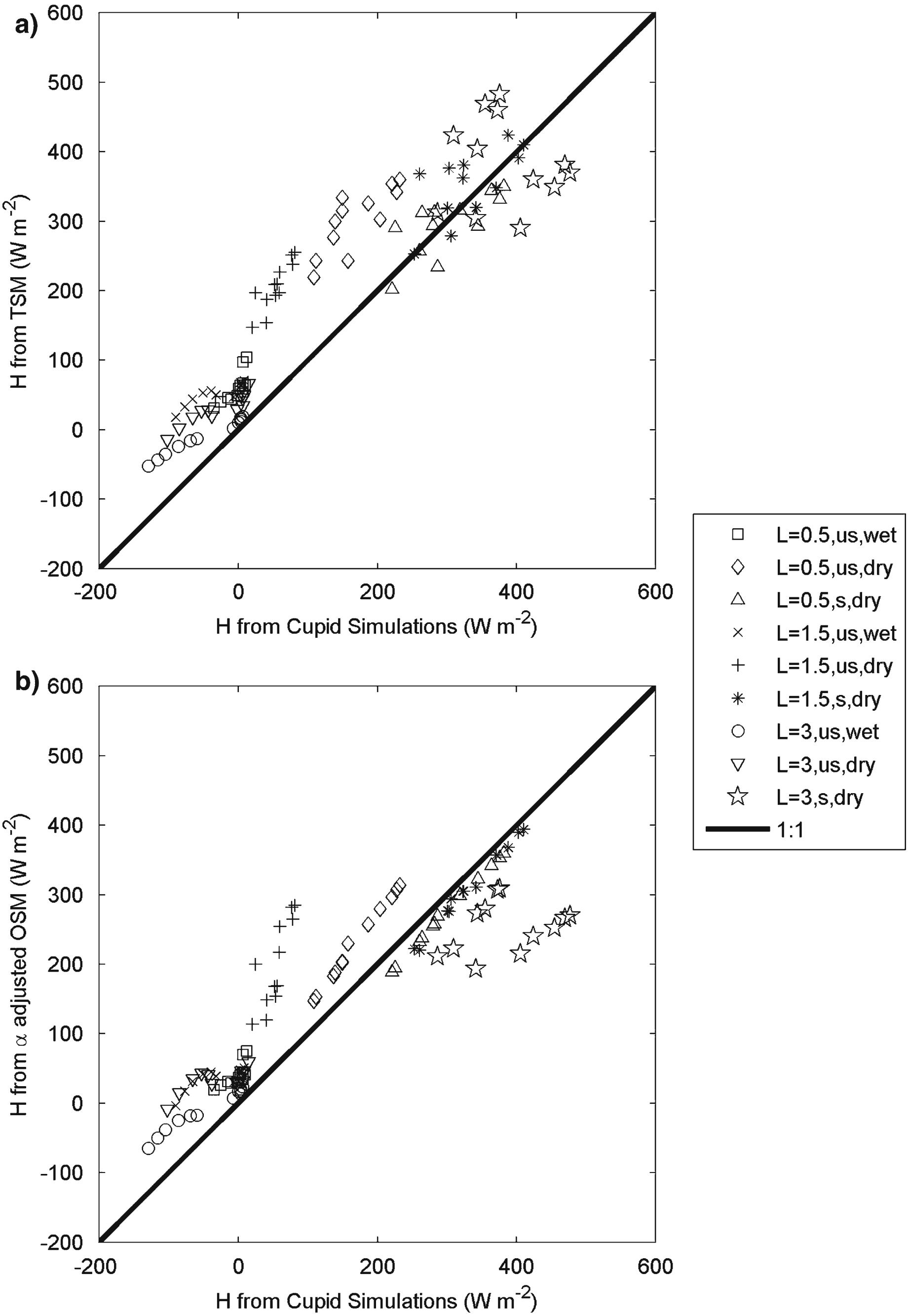


**Fig. 5** Estimates of sensible heat flux $H$ from (**a**) the TSM, and (**b**) the $\alpha$-adjusted OSM versus Cupid simulated output for the different cases (L = LAI, us = unstressed vegetation, s = stressed vegetation, dry = dry soil surface moisture, wet = wet soil surface moisture) with radiometer view angle $\phi = 0°$. Each symbol type contains a range of solar radiation, vapour pressure and air temperature values under the two wind speed conditions ($u = 1$ and $5\,\mathrm{m\,s^{-1}}$). See text for details

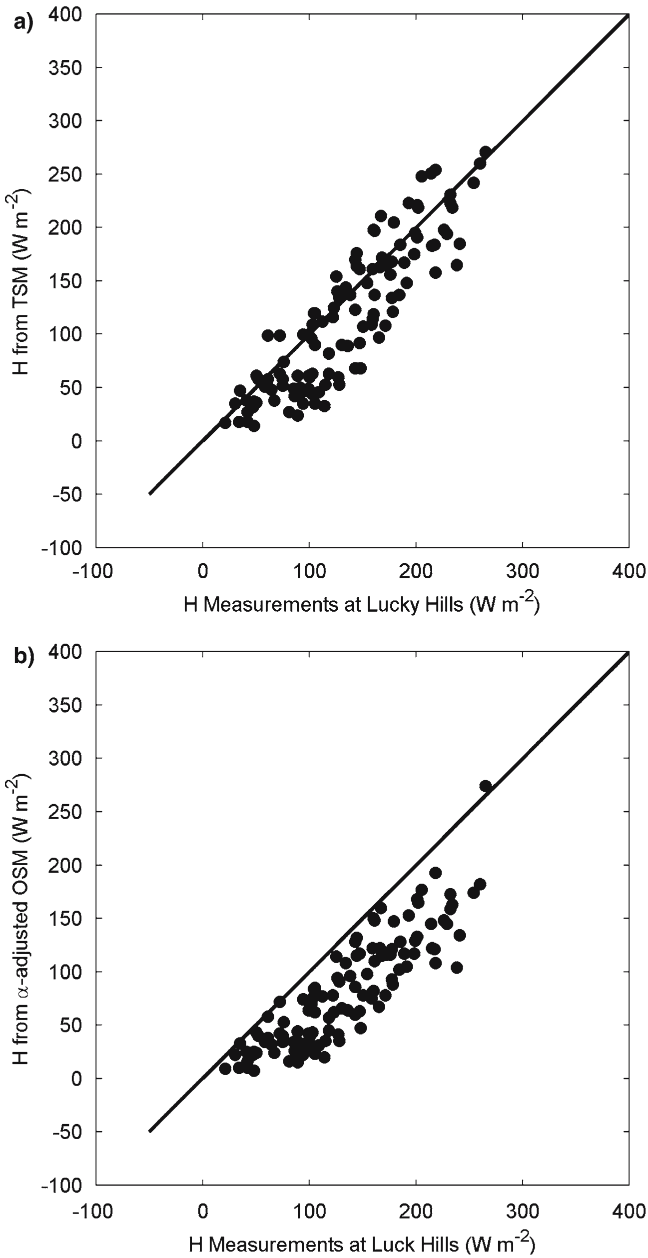


**Fig. 6** Estimates of sensible heat flux $H$ from **(a)** the TSM and (**b**) the $\alpha$-adjusted OSM versus measurements from the Lucky Hills study site collected during Monsoon '90 experiment (see text)

angles (36 cases in all) were used to evaluate the radiometric–aerodynamic temperature difference ($T_R(\phi) - T_O$) formulation proposed by Mahrt and Vickers (2004) and Matsushima (2005). The relation Mahrt and Vickers derived from experimental data over a variety of landscapes suggested a linear expression between $T_R(\phi) - T_O$ and solar radiation, $S$, with the intercept related to leaf area, but essentially a single slope applicable to all sites. The Matsushima adjustment variable $\alpha$ was related to a variation in LAI derived from multi-source canopy model simulations and experimental data from a rice canopy having a wide range in vegetation density.

The Cupid simulations also gave a strong linear relation between $T_R(\phi) - T_O$ and $S$ for individual cases, but both the slope and intercept varied significantly (an order of magnitude or more) between cases. Therefore, it was found that the Mahrt and Vickers (2004) adjustment method does not have general application. In addition, the value of $\alpha$ computed from the Cupid simulations showed significant variation, particularly for LAI = 3. When $T_R(\phi) - T_O$ values were compared to soil–canopy temperature differences, $T_S - T_C$, linear relations with less scatter are observed with the $T_R(\phi) - T_O$ values collapsing along lines (having different slopes) defined by vegetation cover amounts (i.e., LAI $= 0.5, 1.5$ and 3). There was also a difference in slope as a function of radiometer viewing angle (i.e., $\phi = 0°$ and $55°$). This result from the Cupid simulations indicates that having reliable estimates of component soil and canopy temperatures and associated resistances largely defines $T_R(\phi) - T_O$ for a given amount of vegetation cover.

Other studies such as the recent one by Merlin and Chehbouni (2004) (see also Francois 2002) show the benefits of combining dual angle radiometric surface temperature observations with a physically-based two-source modelling scheme for deriving the soil and canopy temperatures. With such two-source approaches that can consider radiometer view angle effects, it is likely that a generalized formulation accommodating differences between radiometric and aerodynamic temperatures for diverse landscapes will be developed.

When appropriately formulated to consider variations in $T_R(\phi) - T_O$, however, one-source approaches may still provide heat flux estimates that are comparable to simplified two-source modelling schemes. This was observed in the present study when sensible heat flux estimates using the two-source model (TSM; Norman et al. 1995; Kustas and Norman 1999) and the one-source model (OSM; Mustushima 2005) using the adjustment variable $\alpha$ were compared to Cupid simulated output. With experimental data (Monsoon '90) from the shrubland site, TSM estimates of $H$ were in better agreement with the observations than the OSM output. This was primarily caused by a significant mean bias (underestimate) in $H$, which could be compensated in part by considering that the vegetation is clumped, reducing the effective LAI. The assumed value for the ratio of roughness lengths for heat and momentum had a much greater effect on the OSM output and could greatly reduce the overall mean bias; however, it resulted in a significant increase in scatter with the observations.

It is important to reiterate the point that the data needs for the TSM approach are essentially the same as OSM schemes. The minimal set of input requirements has allowed the TSM scheme to be implemented in an operational multi-scale land-surface modelling framework operating over the continental U.S. (Diak et al. 2004). This would not be possible with Cupid, which requires numerous input data not readily available.

Moreover, improvements in remote sensing-based flux modelling, such as efforts in combining dual-angle radiometric temperature observations with two-source models (e.g., Merlin and Chehbouni 2004) are more likely to improve the overall reliability of soil and vegetation component temperatures and fluxes than any further refinements of adjustment schemes with one-source approaches. Although regional applications using OSM schemes have also been developed (e.g., Matsushima and Kondo 2000; Su 2002), the ability of the two-source model to separate bulk fluxes into soil and canopy component fluxes (particularly soil evaporation and canopy transpiration) provides more useful information for monitoring vegetation stress and water use (Anderson et al. 2005), and for estimating crop yield (Melesse and Nangia 2005) as well as carbon assimilation (Anderson et al. 2000).

**Acknowledgements** Funding for this research was provided in part by USDA Cooperative Agreement 58-1265-1-043. Comments from the anonymous reviewers improved the manuscript.

## References

Anderson MC, Norman JM, Diak GR, Kustas WP, Mecikalski JR (1997) A two-source time-integrated model for estimating surface fluxes using thermal infrared remote sensing. Remote Sens Environ 60:195–216

Anderson MC, Norman JM, Meyers TP, Diak GR (2000) An analytical model Forest estimating canopy transpiration and carbon assimilation fluxes based on canopy light-use efficiency. Agric Forest Meteorol 101:265–289

Anderson MC, Norman JM, Kustas WP, Li F, Prueger JH, Mecikalski JR (2005) Effects of vegetation clumping on two-source model predictions of surface energy fluxes from an agricultural landscape during SMACEX. J Hydrometeorol 6:892–909

Bland WL, Loew JL, Norman JM (1996) Evaporation from cranberry. Agric for Meteorol 81:1–12

Blümel K (1999) A simple formula for estimation of the roughness length for heat transfer over partly vegetated surfaces. J Appl Meteorol 38:814–829

Blyth EM, Dolman AJ (1995) The roughness length for heat of sparse vegetation. J Appl Meteorol 34:583–585

Bosveld FC, Holtslag AAM, van den Hurk BJJM (1999) Interpretation of crown radiation temperatures of a dense douglas fir forest with similarity theory. Boundary-Layer Meteorol. 92:429–451

Brutsaert W (1975) On a derivable formula for long-wave radiation from clear skies. Water Resour Res 11:742–744

Brutsaert W (1982) Evaporation into the atmosphere. D. Reidel Pub. Co., Dordrecht, Holland, 299 pp

Brutsaert W, Sugita M (1996) Sensible heat transfer parameterization for surfaces with anisothermal dense vegetation. J Atmos Sci 53:209–216

Campbell GS (1985) Soil physics with basic. Elsevier Publ. Co., New York, 150 pp

Chehbouni A, Lo Seen D, Njoku EG, Monteney BM (1996) Examination of the difference between radiometric and aerodynamic surface temperatures over sparsely vegetated surfaces. Remote Sens Environ 58:177–186

Chehbouni A, Lo Seen D, Njoku EG, Lhomme JP, Monteney B, Kerr YH (1997) Estimation of sensible heat flux over sparsely vegetated surfaces: relationship between radiative and aerodynamic surface temperature. J Hydrol 188–189:855–868

Chen JM, Rich PM, Gower ST, Norman JM, Plummer S (1997) Leaf area index of foreal forests: theory, techniques and measurements. J Geophys Res 102(D24):29, 429–443.

Crow WT, Kustas WP (2005) Utility of assimilating surface radiometric temperature observations for evaporative fraction and heat transfer coefficient retrieval. Boundary-Layer Meteorol 115: 105–130

Diak GR, Mecikalski JR, Anderson MC, Norman JM, Kustas WP, Torn RD, DeWolf RL (2004) Estimating land-surface energy budgets from space: review and current efforts at the university of Wisconsin-Madison and USDA-ARS. Bull Amer Meteorol Soc 85(1):65–78

Francois C (2002) The potential of directional radiometric temperatures for monitoring soil and leaf temperature and soil Moisture status. Remote Sens Environ 80:122–133

Friedl MA (2002) Forward and inverse modeling of land surface energy balance using surface temperature measurements. Remote Sens Environ 79:344–354

Garratt JR, Hicks BB (1973) Momentum, heat and water vapor transfer to and from natural and artificial surfaces. Quart J Roy Meteorol Soc 99:680–687

Kustas WP, Goodrich DC (1994) Preface, MONSOON'90 multidisciplinary experiment. Water Resour Res 30:1211–1225

Kustas WP, Norman JM (1996) Use of remote sensing for evapotranspiration monitoring over land surfaces. Hydrol Sci 41:495–516

Kustas WP, Norman JM (1999) Evaluation of soil and vegetation heat flux predictions using a simple two-source model with radiometric temperatures for partial canopy cover. Agric Forest Meteorol 94:13–29

Kustas WP, Norman JM (2000) Evaluating the effects of subpixel heterogeneity on pixel average fluxes. Remote Sens Environ 74:327–342
Kustas WP, Humes KS, Norman JM, Moran MS (1996) Single-and dual-source modeling of surface energy fluxes with radiometric surface temperature. J Appl Meteorol 35:110–121
Kustas WP, Albertson JD, Scanlon TM, Cahill AT (2001) Issues in monitoring evapotranspiration with radiometric temperature observations. In: Owe M, Brubaker K, Ritchie J, Rango A (eds) remote sensing and hydrology 2000, IAHS Publ. No. 267 (ISBN 1-901502-46-5), pp 239–245
Kustas WP, Prueger JH, Hipps LE (2002) Impact of using different time-averaged inputs for estimating sensible heat flux of riparian vegetation using radiometric surface temperature. J Appl Meteorol 41:319–332
Kustas WP, Norman JM, Schmugge TJ, Anderson MC (2004) mapping surface energy fluxes with radiometric temperature. In: Quattrochi D, Luvall J (eds) Thermal remote sensing in land surface processes. CRC Press, Boca Raton, FL, pp 205–253
Lhomme J-P, Monteny B, Amadou M (1994) Estimating sensible heat flux from radiometric temperature over sparse millet. Agric for Meteorol 68:77–91
Lhomme J-P, Troufleau D, Monteny B, Chehbouni A, Bauduin S (1997) Sensible heat flux and radiometric surface temperature over sparse sahelian vegetation II: a model for the $kB^{-1}$ parameter. J Hydrol 188–189:839–854
Mahrt L, Vickers D (2004) Bulk formulation of the surface heat flux. Boundary-Layer Meteorol 110:357–379
Mahrt L, Sun J, MacPherson JI, Jensen NO, Desjardins RL (1997) Formulation of the surface temperature for prediction of heat flux:application to BOREAS. J Geophys Res 102:641–649
Massman W (1999) A model study of $kB_H^{-1}$ for vegetated surfaces using 'localized near-field Lagrangian' Theory. J Hydrol 223:27–43
Matsushima D (2005) Relations between aerodynamic parameters of heat transfer and thermal-infrared thermometry in the bulk surface formulation. J Meteorol Soc Japan 83:373–389
Matsushima D, Kondo J (1997) A proper method for estimating sensible heat flux above a horizontal-homogeneous vegetation canopy using radiometric surface observations. J Appl Meteorol 36:1696–1711
Matsushima D, Kondo J (2000) Estimating regional distribution of sensible heat flux over vegetation using satellite infrared temperature with view angle correction. J Meteorol Soc Japan 78:753–763
McNaughton KG, Van den Hurk BJJM (1995) A 'Lagrangian' revision of the resistors in the two-layer model for calculating the energy budget of a plant canopy. Boundary-Layer Meteorol 74:262–288
Melesse AM, Nangia V (2005) Estimation of spatially distributed surface energy fluxes using remotely-sensed data for agricultural fields. Hydrol Proc 19:2653–2670
Merlin O, Chehbouni A (2004) Different approaches in estimating heat flux using dual angle observations of radiative surface temperature. Int J Remote Sensing 25(1):275–289
Norman JM (1979) Modeling the complete crop canopy. In: Barfield BJ, Gerber JF (eds) Modification of the aerial environment of plants, ASAE Monogr Am Soc Agric Engr, St. Joseph, MI, pp 249–277
Norman JM (1988) Synthesis of canopy processes. In: Russell G. et al. (eds) plant canopies: their growth, form and function, Soc. Exp. Biol, Seminar Series 31, Cambridge University Press, New York, pp 161–175
Norman JM, Arkebauer TJ (1991) Predicting canopy light-use efficiency from leaf characteristics. In: Ritchie JT, Hanks RJ (eds) Modeling plant and soil systems. ASA Society, Madison, WI, pp 125–143
Norman JM, Becker F (1995) Terminology in thermal infrared remote sensing of natural surfaces. Remote Sens Rev 12:159–173
Norman JM, Campbell GS (1983) Application of a plant-environment model to problems in irrigation. In: Hillel DI (ed) Advances in irrigation, vol. II, Academic Press, New York, pp 155–188
Norman JM, Jarvis PG (1975) Photosynthesis in sitka spruce (Picea sichensis (Bong.) Carr.): IV. Radiation penetration theory and a test case. J Appl Ecol 12:839–878
Norman JM, Polley W (1989) Canopy photosynthesis. In: Briggs WR (ed) Photosynthesis. Alan R. Liss, Inc., New York, pp 227–241
Norman JM, Welles JM, Walter EA (1985) Contrasts among bidirectional reflectance of leaves, canopies and soils. IEEE Trans Geosci Remote Sen GE-23, 659–667
Norman JM, Kustas WP, Humes KS (1995) A two-source approach for estimating soil and vegetation energy fluxes from observations of directional radiometric surface temperature. Agric Forest Meteorol 77:263–293

Raupach MR (1994) Simplified expressions for vegetation roughness length and zero-plane displacement as functions of canopy height and area index. Bound.-Layer Meteorol 71:211–216, Corrigenda 76:303–304
Shuttleworth WJ, Wallace JS (1985) Evaporation From sparse canopies–an energy combination theory. Quart J Royal Meteorol Soc 111:839–855
Stannard DI, Blanford JH, Kustas WP, Nichols WD, Amer SA, Schmugge TJ, Weltz MA (1994) Interpretation of surface- flux measurements in heterogeneous terrain during the MONSOON 90 Experiment. Water Resour Res 30(5):1227–1239
Stewart JB, Kustas WP, Humes KS, Nichols WD, Moran MS, De Bruin AAR (1994) Sensible heat flux-radiometric surface temperature relationship for eight semiarid areas. J Appl Meteorol 33:1110–1117
Su Z (2002) The surface energy balance system (SEBS) for estimation of turbulent heat fluxes. Hydrol Earth Sys Sci 6:85–99
Su Z, Schmugge T, Kustas WP, Massman WJ (2001) An evaluation of two models for estimation of the roughness height for heat transfer between the land surface and the atmosphere. J Appl Meteorol 40:1933–1951
Sun J (1999) Diurnal variations of thermal roughness height over a grassland. Boundary-Layer Meteorol 92:407–427
Sun J, Mahrt L (1995) Determination of surface fluxes from the surface radiative temperature. J Atmos Sci 52:1096–1106
Sun J, Massman W, Grantz D (1999) Aerodynamic variables in the bulk formula. Boundary-Layer Meteorol 91:109–125
Troufleau D, Lhomme JP, Monteney B, Vidal A (1997) Sensible heat flux and radiometric surface temperature over sparse sahelian vegetation. I. An experimental analysis of the $kB^{-1}$ parameter. J Hydrol 188–189:815–838
Verhoef A, De Bruin HAR, van den Hurk BJJM (1997) Some practical notes on the parameter $kB^{-1}$ for sparse vegetation. J Appl Meteorol 36:560–572
Vining RC, Blad BL (1992) Estimation of sensible heat flux from remotely sensed canopy temperatures. J Geophys Res 97(D17):18951–18954
Weiss A, Lukens EL, Norman JM, Steadman JR (1989) Leaf wetness in dry beans under semi-arid conditions. Agric Forest Meteorol 48:49–162
Willmott CJ (1982) Some comments on the evaluation of model performance. Bull Amer Meteorol Soc 11:1309–1313
Wilson TB, Bland BL, Norman JM (1999) Measurement and simulation of dew accumulation and drying in a potato canopy. Agric Forest Meteorol 93:111–119
Wilson TB, Norman JM, Bland WL, Kucharik CJ (2003) Evaluation of the importance of 'lagrangian' canopy turbulence formulations in a soil-plant-atmosphere model. Agric Forest Meteorol 115:51–69
Zhan X, Kustas WP, Humes KS (1996) An intercomparison study on models of sensible heat flux over partial canopy surfaces with remotely sensed surface temperature. Remote Sens Environ 58:242–256